Article

BcAMT1;5 Mediates Nitrogen Influxes in Flowering Chinese Cabbage and Improves Plant Growth when Overexpressed in *Arabidopsis*

Yunna Zhu [1,2,#], Lihua Zhong [2,3,#], Xinmin Huang [2,4], Wei Su [2], Houcheng Liu [2], Guangwen Sun [2], Shiwei Song [2,*], and Riyuan Chen [2,*]

[1] Henry Fok College of Biology and Agriculture, Shaoguan University, Shaoguan, 512005, Peoples R China
[2] College of Horticulture, South China Agricultural University, Guangzhou, 510642, Peoples R China
[3] College of Agriculture and Food Engineering, Baise University, Baise, 533000, Peoples R China
[4] College of Biology and Food Engineering, Guangdong University of Petrochemical Technology, Maoming, 525000, Peoples R China

# These authors contributed equally to this work.
* Correspondence: SS-swsong@scau.edu.cn; Tel.: +86-20-85280228; RC-rychen@scau.edu.cn; Tel.: +86-20-38294595

Abstract: Nitrogen (N) is a major limiting factor for plant growth and vegetable production. Understanding the regulatory mechanisms of N uptake, transport, and assimilation is key to improving nitrogen use efficiency in plants. Ammonium transporters (AMTs) play an important role in plant N metabolism. In this study, we isolated an important AMT1 subfamily member (*BcAMT1;5*) with a highly conserved signatural AMT1 subfamily motif from flowering Chinese cabbage. Based on functional complementation in yeast mutant 31019b and overexpression of *BcAMT1;5* in *Arabidopsis*, BcAMT1;5 is a functional ammonium transporter. Tissue expression analysis showed that *BcAMT1;5* was mainly expressed in roots and showed multiple N regime transcript patterns to respond to varying nutritional conditions. This was up-regulated by N-deficiency and down-regulated by supplying NH_4^+. The glucuronidase (GUS) activities of *BcAMT1;5*$_{pro}$*::GUS* showed a similar change in response to different N conditions. Overexpression of *BcAMT1;5* accelerated the growth of transgenic seedlings, increased NH_4^+ net influxes, and enhanced the content and accumulation of NH_4^+ and NO_3^- at low N concentrations. Additionally, it increased the transcript levels of N assimilation-related genes in shoots. These results indicate that the transcriptional regulation of *BcAMT1;5* in flowering Chinese cabbage may participate in N uptake and assimilation under various N conditions.

Keywords: ammonium transport; flowering Chinese cabbage; NH_4^+; NO_3^-; ion influx; overexpression

1. Introduction

Nitrogen (N) is pivotal to the yield and quality of vegetables, and the application of N fertilizer in vegetable production systems is a crucial aspect of modern vegetable management practices and one of the determining factors to increase vegetable yield, thereby keeping pace with the increase in the human population [1]. However, most of the N fertilizers (>60%) added to fields are not taken up by plants but are lost to the environment in the form of ammonia, nitrate (NO_3^-), and nitrous oxide. NO_3^- and ammonium (NH_4^+) are major sources of inorganic N. Most plants preferentially use NO_3^- as the N source, and its reduction is inhibited by elevated carbon dioxide (CO_2); however, NH_4^+ assimilation is hardly affected [2]. Because NH_4^+ can be directly assimilated via the glutamine synthetase (GS) and NADH-dependent glutamate synthase (GOGAT) pathways, NH_4^+ plays a key role in plant symbiosis [3], especially when plants suffer to N-deficiency because they

Preprints (www.preprints.org) | NOT PEER-REVIEWED | Posted: 16 November 2022 doi:10.20944/preprints202211.0305.v1

require less energy for assimilation [4]. However, excess NH_4^+ can be toxic to plants [5]. Consequently, the absorption and transport of NH_4^+ must be regulated in plants.

Ammonium transporters on the plasma membranes of root cells transport NH_4^+ into plants [6]. Ammonium transporters, which include the superfamily of ammonium transporter (AMT), methylamine permease (MEP), and rhesus factor protein (Rh), mainly mediate the acquisition and transport of NH_4^+ to supply NH_4^+ nutrients for plants or microorganisms. The MEP and Rh proteins are mainly found in fungi, bacteria, and animals, whereas AMT is found in plants and animals [7]. In plants, the AMT family is divided into two subfamilies: AMT1 and AMT2 [6, 7]. Most AMT1 subfamily genes, as high-affinity members, respond to N starvation. In *Arabidopsis*, the AMT1 subfamily includes AtAMT1;1–AtAMT1;5, AtAMT1;1, AtAMT1;2, and AtAMT1;3, which contribute to approximately 90% of the total high-affinity NH_4^+ uptake capacity in roots, and AtAMT1;5 contributes to the rest [8]. The AtAMT1;1, AtAMT1;3, and AtAMT1;5 proteins mainly participate in absorbing ammonium from soil; *AtAMT1;2* mediates NH_4^+ uptake by root cells via the apoplasmic transport route [8]; and AtAMT1;4 functions in transporting NH_4^+ into pollen [9]. This indicates that all AtAMT proteins have different roles in absorption and transport, displaying distinct ammonium transport affinities and capacities [10].

In maize, the expression of *ZmAMT1;1a* and *ZmAMT1;3* is induced by resupplying NH_4^+ into N-deficient roots and promoting NH_4^+ absorption [11]. In rice, the expression of *OsAMT1;1*, *OsAMT1;2*, and *OsAMT1;3* is cooperatively regulated by the uptake of low ammonium; however, they undergo different regulatory mechanisms [12]. In apples, both *AMT1;2* and *AMT1;5* are induced by N-deficiency, while *AMT1;2* is up-regulated by NH_4^+-resupply and *AMT1;5* is decreased by NH_4^+ resupply. The *AMT1;5* gene has the highest transcript levels in young fruits and is up-regulated at an early stage, suggesting that it may play a role in providing ammonium nutrition during fruit development [13]. In flowering Chinese cabbage, *BcAMT1;2* is up-regulated by NH_4^+ and NO_3^-, especially a mixture of NH_4^+ and NO_3^-, and mediates the interaction between NH_4^+ and NO_3^- [14]. However, the same homologous genes from different plants or genes from the same plant exhibit different expression characteristics. For example, AtAMT1;4 participates in NH_4^+ transport in pollen with a higher mRNA abundance in *Arabidopsis* pollen [9], whereas BcAMT1;4 mainly participates in leaf ammonium transport [15]. The AMT1 proteins appear to have different mechanisms depending on their physiological roles [16].

Most studies on AMTs are concerned with AMT1;1, AMT1;2, and AMT1;3, and very little information concerning the function of AMT1;5 exists. Thus, in the present study, an AMT1-type gene, *BcAMT1;5*, was isolated from flowering Chinese cabbage (*Brassica campestris* L. ssp. *chinensis* var. *utilis* Tsen et Lee), and its expression characteristics and functions were analyzed.

2. Results

2.1. Molecular Identification of AMT1;5 Homolog from Flowering Chinese Cabbage

To explore the molecular components of AMT1;5 in flowering Chinese cabbage, the *Arabidopsis AtAMT1; 5* sequence [8] was used as a reference to search for homologs in the *Brassica rapa* genomic database. We obtained a homologous sequence using cDNA from flowering Chinese cabbage, designated *BcAMT1;5* (GenBank accession number: MF966940), the ORF of which was 1503 bp in length, encoding a protein of 500 amino acids, with a predicted molecular weight of 53.17 kDa and an isoelectric point of 6.24.

Phylogenetic analysis was performed based on the amino acid sequences of the AMT1 and AMT2 subfamily members from *Arabidopsis thaliana*, *Brassica rapa*, *Oryza sativa*, and *Populus trichocarpa*. This shows that BcAMT1;5 belongs to the AMT1 cluster and is highly homologous to AMT1;5 from *Arabidopsis* and *B. rapa*, which share 91.00% and 99.60% sequence identity, respectively (Figure 1A, B). The BcAMT1;5-coding protein is predicted to be an integral membrane protein with 10 transmembrane domains (TMs) with both the N-terminus and C-terminus inside the cytoplasm, with a signature motif of the AMT1 subfamily in the 6th TMs (red box in Figure 1B). Overall, these results indicate

Preprints (www.preprints.org) | NOT PEER-REVIEWED | Posted: 16 November 2022 doi:10.20944/preprints202211.0305.v1

that BcAMT1;5 is a member of the AMT1 subfamily, which has been identified in flowering Chinese cabbage.

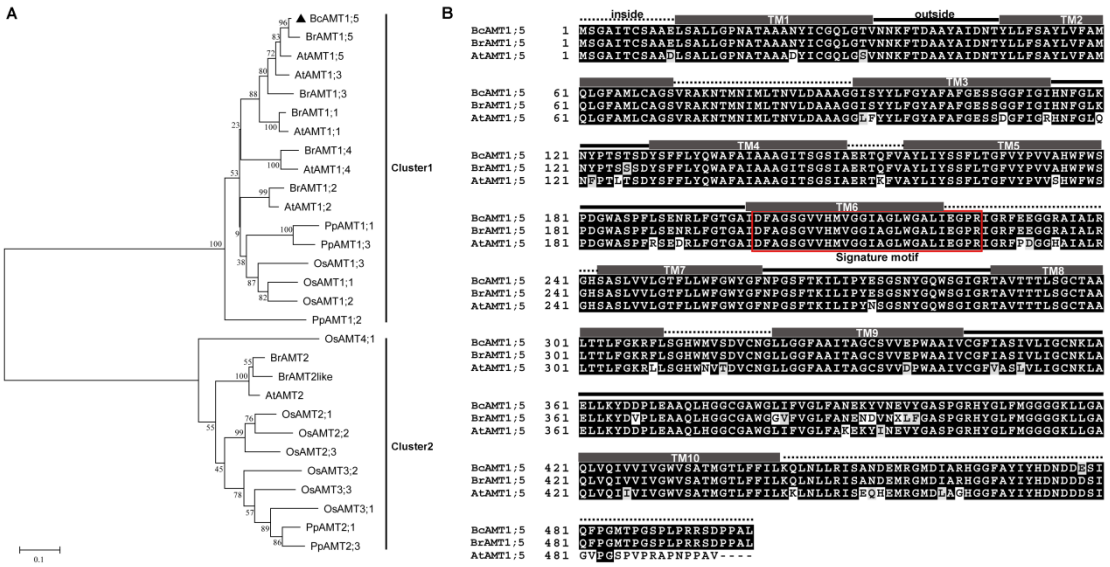

Figure 1. Phylogenetic tree of ammonium transporter (AMT) homologs and amino acid sequences alignment of AMT1;5 from *Brassica campestris*, *B. rapa* and *Arabidopsis*. A: The phylogenetic tree of AMT family proteins was constructed using the Neighbor-Joining method in MEGA 6.0. Bootstrap values were from 1000 replications, the numbers at the nodes are bootstrap values. Accession numbers of AMTs protein were listed in Table S1. At, *Arabidopsis thaliana*; Bc, *Brassica campestris*; Br, *Brassica rapa*; Os, *Oryza sativa*; Ptr, *Populus trichocarpa*. BcAMT1;5 from *B. campestris* is marked by a black triangle. The sequence information for each protein is provided in Table S2. B: Sequence alignment of BcAMT1;5, BrAMT1;5, and AtAMT1;5 performed by using CloustalW in MEGA 6.0. Amino acids are shown with standard single-letter designations; identical residues are presented in white letters on black at the aligned positions of two or three sequences. Gray boxes above the sequences show the positions of 10 potential transmembrane domains (TMs), and the connecting lines indicate putative inside- and outside-cytoplasm domains, as predicted by TMHMM 2.0 (http://www.cbs.dtu.dk/services/TMHMM/). The sequences marked in the red box indicate the signature motif of the AMT1 subfamily identified by Couturier et al. [17].

2.2. Subcellular Localization of BcAMT1;5 and its Functional Complementation Analysis in Yeast Mutant Cells

Using the petiole epidermis of the instantaneously overexpressing *pBI121-BcAMT1;5-GFP* in onion, we observed that the green fluorescent protein (GFP) signal was mainly localized in the plasma membrane (Figure 2).

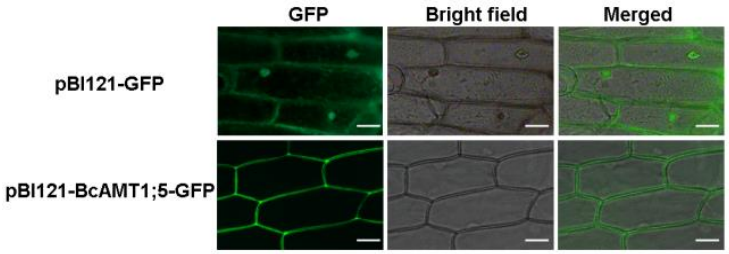

Figure 2. Subcellular localization of pBI121-GFP, pBI121-BcAMT1;5-GFP fusion proteins in onion epidermal cells. Bright field: image obtained by bright field microscopy; GFP: green fluorescence derived from GFP imaged by fluorescence microscopy; Merged: overlay of the two images. Scale bar: 50 μm.

To rapidly test the putative molecular functionality of BcAMT1;5 in the transportation of ammonium, the ORF of *BcAMT1;5* was cloned into the yeast expression vector pYES2 and then transformed into the yeast mutant strain 31019b. It cannot grow on

Preprints (www.preprints.org) | NOT PEER-REVIEWED | Posted: 16 November 2022 doi:10.20944/preprints202211.0305.v1

medium containing an ammonium concentration lower than 5 mmol L^{-1} as the sole N source [8]. Recombinant yeast strains harboring the empty vector (pYES2) hardly grew and those harboring pYES2-BcAMT1;5 grew normally on medium containing 2 mmol L^{-1} NH_4^+ as the sole N source. Both recombinant yeast strains harboring pYES2-BcAMT1;5 and pYES2 grew normally on medium containing 2 mmol L^{-1} arginine (Figure 3). This indicated that BcAMT1;5 complemented the defect in the yeast mutant strain 31019b, which cannot grow on medium with less than 5 mmol L^{-1} NH_4^+ as the sole N source, suggesting that BcAMT1;5 is a functional ammonium transporter.

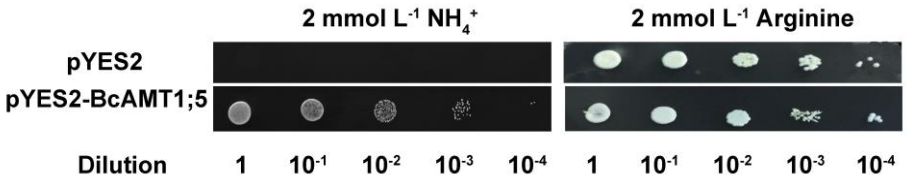

Figure 3. Functional complementation of yeast mutant 31019b cells by *BcAMT1;5*. pYES2: empty vector was used as the negative control. pYES2-BcAMT1;5: ORF of *BcAMT1;5* was cloned into pYES2 vector. Yeast cell suspensions were adapted to an optical density at 600 nm of 1.0 (dilution 1). Then, they were serially diluted by factors of 10, and 3 μL of the yeast cell suspensions at each dilution were spotted on yeast nitrogen base medium. Growth was evaluated after three days of incubation at 30 °C.

2.3. Expression Profiles for BcAMT1;5 Gene in Different Tissues of Flowering Chinese Cabbage

To further characterize *BcAMT1;5* in flowering Chinese cabbage, its expression patterns were investigated in the roots, leaves, stems, petioles, and flowers. The *BcAMT1;5* gene was expressed most highly in the roots and flowers, and either low-level transcripts or no transcripts were detected in the leaf, stem, and petioles (Figure 4). Thus, the expression patterns of *BcAMT1;5* were analyzed only in the roots in the following experiments.

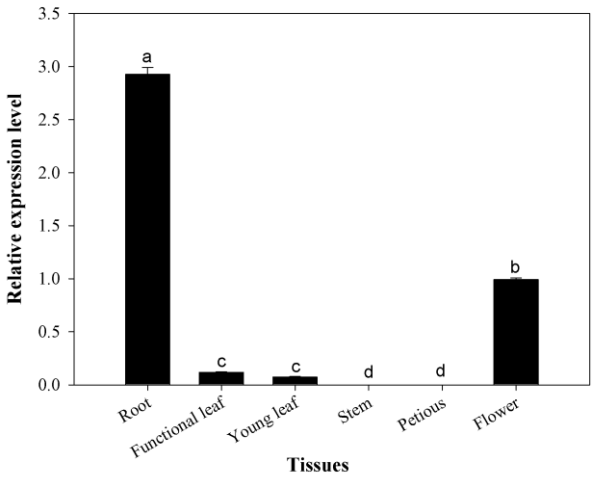

Figure 4. *BcAMT1;5* expression patterns in different organs of flowering Chinese cabbage. Each value represents the mean ± SE (n=3). Different lowercase letters show significant differences at $p < 0.05$.

2.4. Expression Profiles for BcAMT1;5 Gene in Different N Regimes

Flowering Chinese cabbage seedlings were precultured in hydroponic nutrient solutions supplemented with 4 mmol L^{-1} NO_3^- as the sole N source for 12 d and then transferred to N-free nutrient solutions. The N-starvation treatment increased the transcription level of *BcAMT1;5* in the roots, with an increase in the time of N-starvation treatment, with the highest level occurring 48 h after the N starvation treatment, and this was almost 5.69 times higher than that at 0 h (Figure 5).

Preprints (www.preprints.org) | NOT PEER-REVIEWED | Posted: 16 November 2022 doi:10.20944/preprints202211.0305.v1

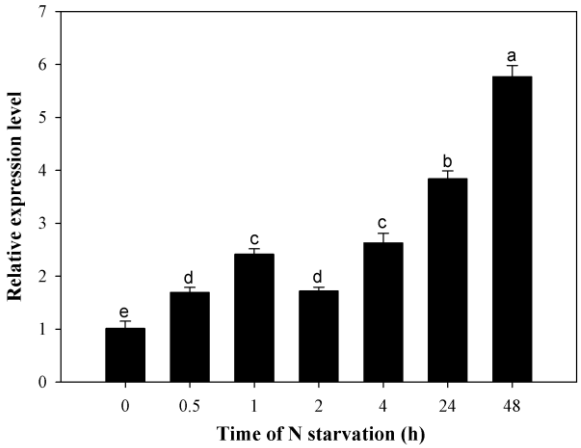

Figure 5. *BcAMT1;5* expression in response to N starvation for 0, 0.5, 1, 2, 4, 24, and 48 h. Each value represents the mean ± SE (n=3). Different lowercase letters show significant differences at $p < 0.05$.

To determine the molecular response of *BcAMT1;5* to plant N status, its expression levels were investigated using qPCR. After N starvation for 48 h, *BcAMT1;5* expression in roots was slightly increased at the level of 0.5 mmol L^{-1} NH_4^+ for 2 h, while it was evidently decreased at the levels of 2 and 10 mmol L^{-1} NH_4^+, being 67.60% and 77.83% of the control (Figure 6A). When adding different concentrations of NH_4^+ at normal N levels, the transcript levels of *BcAMT1;5* were sharply inhibited, with levels of 13.97–65.67% of control grown with normal N supply (Figure 6B). Therefore, the addition of NH_4^+ inhibited the expression of *BcAMT1;5* in flowering Chinese cabbage and increased it with NH_4^+ concentration. Similarly, supplying different ratios of NH_4^+ and NO_3^- nutrition clearly affected the transcription levels of *BcAMT1;5* in flowering Chinese cabbage (Figure 6C, D). After N starvation for 48 h, the addition of NH_4^+ and the mixture of NH_4^+ and NO_3^- decreased *BcAMT1;5* expression compared with that of sole NO_3- treatment (Figure 6C). However, at normal N levels, adding the ratios of NH_4^+ to NO_3^- at 5:95 and 25:75, up-regulated *BcAMT1;5* transcription, and adding the ratios of 50:50 and 100:0 significantly down-regulated its expression level at the level of 0.05 (Figure 6D). These results indicated that *BcAMT1;5* transcription was obviously affected by the external environment N constitution, i.e., N-deficiency, NH_4^+ concentration, and the ratios of NH_4^+ and NO_3^- nutrition.

Preprints (www.preprints.org) | NOT PEER-REVIEWED | Posted: 16 November 2022 doi:10.20944/preprints202211.0305.v1

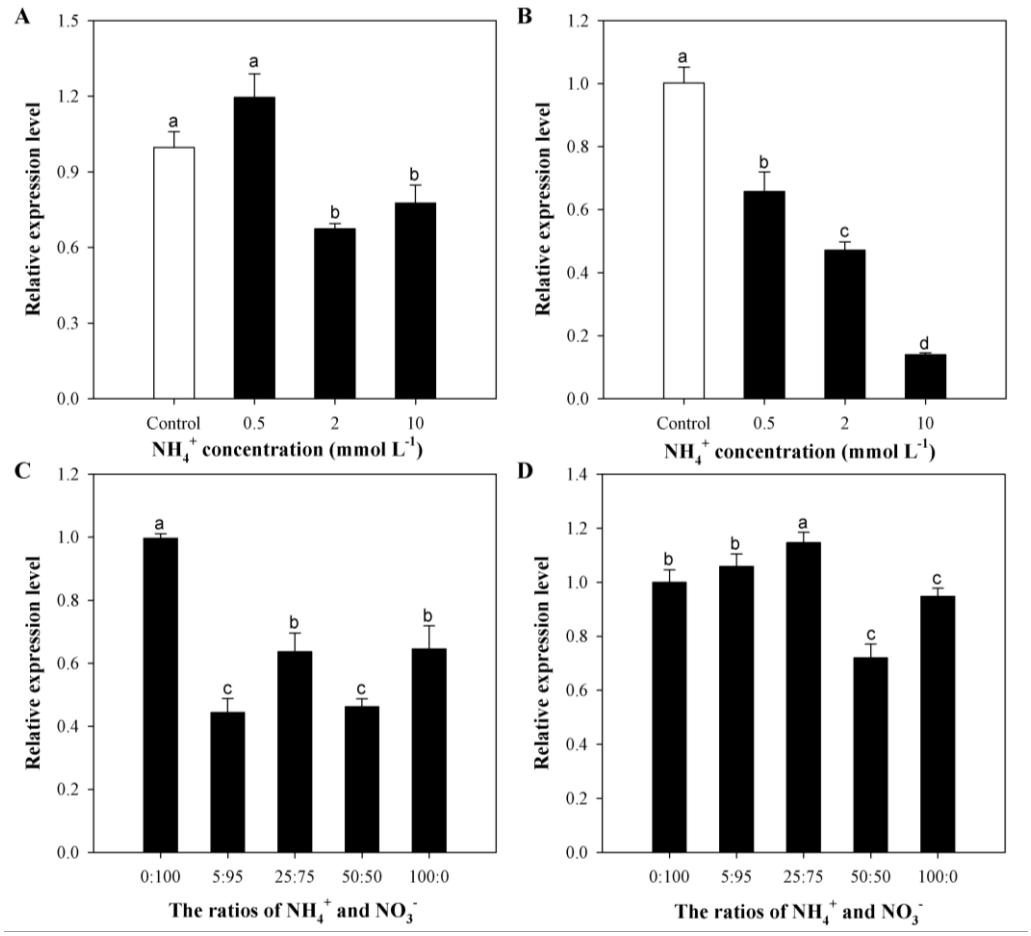

Figure 6. *BcAMT1;5* expression patterns in root of flowering Chinese cabbage in response to different nitrogen (N) regimes. *BcAMT1;5* expression in response to 0, 0.5, 2, and 10 mmol L^{-1} NH_4^+ for 2 h after N-deficiency for 48 h. (**A**) and at the normal N level (4 mmol L^{-1} NO_3^-) (**B**). *BcAMT1;5* expression in response to different ratios of NO_3^- and NH_4^+ nutrition (the total N = 4 mmol L^{-1}) for 2 h after N-starvation for 48 h (**C**) and at the normal N level (**D**). Values and error bars indicate the mean ± SE (n=3). Different lowercase letters indicate significant differences at $p < 0.05$.

2.5. Expression of BcAMT1;5 Gene in Light Regimes

The transcript of *BcAMT1;5* exhibited diurnal rhythms, showing that *BcAMT1;5* had greater expression during the light period than during the dark period, with the lowest expression at 00:00 and the highest at 12:00 (about 3.71–fold that observed at 00:00) (Figure 7). This indicates that the transcript of *BcAMT1;5* in flowering Chinese cabbage has a circadian rhythm.

Preprints (www.preprints.org) | NOT PEER-REVIEWED | Posted: 16 November 2022 doi:10.20944/preprints202211.0305.v1

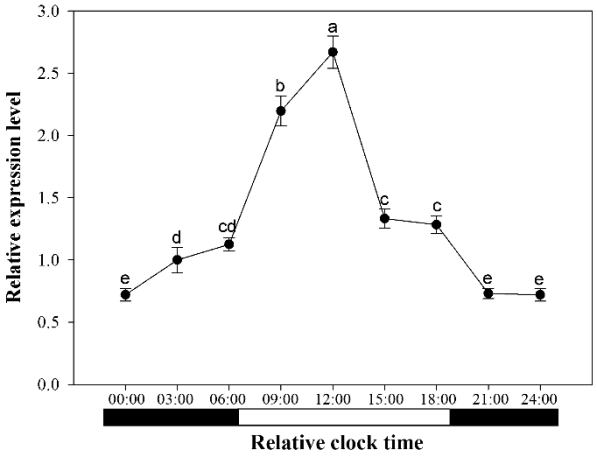

Figure 7. *BcAMT1;5* expression in response to circadian rhythm and light intensity in flowering Chinese cabbage roots. Seedlings were grown in normal nutrient solution, 150 μmol m^{-2} s^{-1} light intensity and a 12h/12h light/dark period (light, 7:00 to 19:00; dark 19:00 to 7:00). Roots were collected at 3 h intervals. Black boxes represent the dark period, the white boxes represent the light period. Values and error bars indicate mean ± SE (*n*=3). Different lowercase letters show significant differences at $p < 0.05$.

2.6. The GUS Activities of BcAMT1;5$_{pro}$::GUS in Response to Different N Conditions

To further understand the expression levels of *BcAMT1;5* under different N forms, we isolated the promoter of *BcAMT1;5* (*BcAMT1;5$_{pro}$*) and constructed the fusion vector of *BcAMT1;5$_{pro}$* and pCAMBIA1391 empty vector, in which the *GUS* gene is not driven by any promoter. Histochemical staining of *pCAMBIA1391-BcAMT1;5$_{pro}$::GUS* transformants was performed in response to different N treatments, being N-free, NH_4^+, NO_3^-, and a mixture of NH_4^+ and NO_3^-. The GUS activity of *pCAMBIA1391* empty vector did not change under N forms, while those of *BcAMT1;5$_{pro}$* showed significant changes in response to different N treatments. Its GUS activities were enhanced in response to N-free and NO_3^- treatments, and decreased in response to NH_4^+ or the mixture of NH_4^+ and NO_3^-, especially NH_4^+. The GUS staining was mainly observed in the vascular tissues of the roots and shoots (Figure 8).

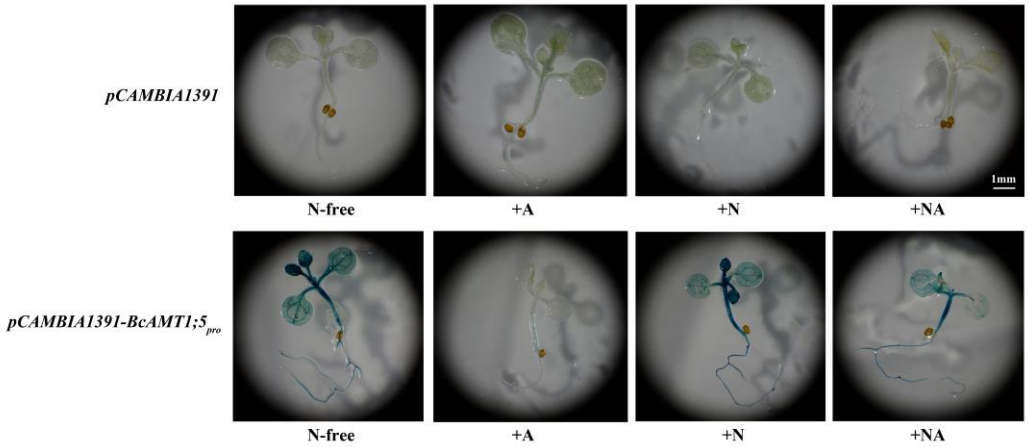

Figure 8. Histochemical staining for glucuronidase (GUS) activities in *Arabidopsis* seedlings transformed with *pCAMBIA1391-BcAMT1;5$_{pro}$::GUS*. Transgenic seedlings were subjected to N-free treatment for 4 d, and supplied with 0.25 mmol L^{-1} NH_4^+, 0.25 mmol L^{-1} NO_3^-, a mixture of 0.1875 mmol L^{-1} NO_3^- , and 0.0625 mmol L^{-1} NH_4^+ for 2 h after N-free treatment. +A, +N, and +NA indicate NH_4^+, NO_3^-, and the mixture of NO_3^- and NH_4^+, respectively.

Preprints (www.preprints.org) | NOT PEER-REVIEWED | Posted: 16 November 2022 doi:10.20944/preprints202211.0305.v1

2.7. Heterologous Expression of BcAMT1;5 in Arabidopsis

To gain insight into the potential role of BcAMT1;5 in plants, *BcAMT1;5* was overexpressed in *the Arabidopsis* wild-type line (Col-0), which provides 0.25 mmol L^{-1} NH_4^+ as the sole N-source. Several independent homozygous lines harboring *BcAMT1;5* were constructed and the expression of *BcAMT1;5* in *Arabidopsis* was confirmed by qPCR (Figure S1). The seedlings were precultured at 4 mmol L^{-1} NO_3^- for 4 d and grown for 10 d on vertical agar plates containing 0.25 mmol L^{-1} NH_4^+. The growth phenotype of transgenic lines showed that overexpression of *BcAMT1;5* in *Arabidopsis* obviously promoted the growth of seedlings at 0.25 mmol L^{-1} NH_4^+. The fresh weight of shoots and roots was significantly increased in most overexpression lines (Figure 9B), and the length of the primary root was increased (Figure 9C). Compared with the wild-type, transgenic lines had significantly increased NH_4^+ content (Figure 9D). Based on the result of NH_4^+ influx, ox-6 significantly increased the net NH_4^+ ion influx by 1.48-fold (Figure 9E).

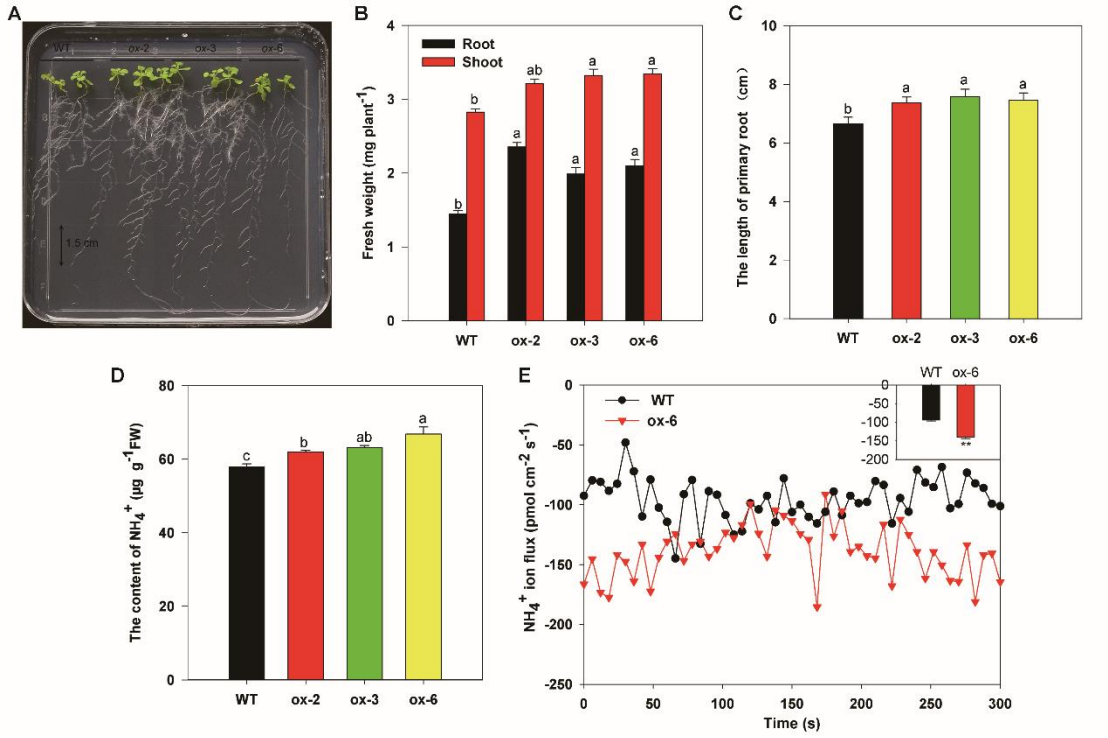

Figure 9. Overexpression of *BcAMT1;5* in A*rabidopsis* improves plant growth at 0.25 mmol L^{-1} of NH_4^+ as an N source. (**A**) The growth phenotype of T_4 transgenic lines together with wild-type at low NH_4^+ levels. Seedlings were grown vertically on solid medium containing 0.25 mmol L^{-1} NH_4^+ for 10 d after a 4-d preculture on 4 mmol L^{-1} NO_3^-. (**B**) Fresh weight of wild-type, and the lines of overexpressing vector and *BcAMT1;5*. (**C**) The length of primary root of wild-type, and the lines of overexpressing *BcAMT1;5*. (**D**) NH_4^+ content of whole plants of wild-type, and the lines of overexpressing *BcAMT1;5*. (**E**) NH_4^+ ion flux of wild-type and the line 6 of overexpressing *BcAMT1;5*. WT: wild-type, ox-2, ox-3, and ox-6 present the line 2, 3, and 6 of overexpressing *BcAMT1;5*, respectively. Line chart: time series plot of NH_4^+ fluxes; histogram: diagram of NH_4^+ fluxes. Data represent mean ± SE (n = 10 in A, B, C; n = 3 in D; n = 6 in E), different letters above the bars indicate significant differences at $p < 0.05$, and ** in the histogram shows significant differences at $p < 0.01$.

To further evaluate the function of *BcAMT1;5*, NH_4^+ resistance of overexpressing *BcAMT1;5 Arabidopsis* was transferred to 20 mmol L^{-1} methylammonium (MeA), a toxic analog of NH_4^+. As shown in Figure 10A, the growth of seedlings was weaker in each line overexpressing *BcAMT1;5* than in the wild-type, with the shortened primary root length and the yellower shoot. Compared with the fresh weight of the wild-type, the fresh weight of the transgenic lines was sharply reduced, being 38.46–59.36% (Figure 10B). Therefore, overexpression of *BcAMT1;5* in *Arabidopsis* significantly inhibited the growth of seedlings,

Preprints (www.preprints.org) | NOT PEER-REVIEWED | Posted: 16 November 2022 doi:10.20944/preprints202211.0305.v1

showing symptoms of NH_4^+ toxicity (i.e., shorting roots and yellowish leaves). This indicates that the *BcAMT1;5*-overexpressed lines enhanced the absorption of NH_4^+.

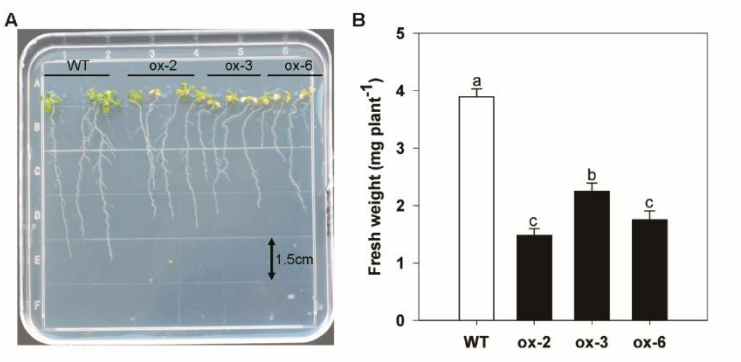

Figure 10. The growth phenotype and fresh weight of the whole plants of overexpressing *BcAMT1;5* on NH_4^+ toxic analog methylammonium (MeA). (**A**) Growth of wild-type and transgenic lines (line 2, 3, 6) on agarose containing 20 mmol L^{-1} MeA for 10d after being precultured 4 mmol L^{-1} NO_3^- for 4 d. (**B**) Fresh weight of the same plants as shown in (A). WT: wild-type, ox-2, ox-3, and ox-6 present the line 2, 3, and 6 of overexpressing *BcAMT1;5*, respectively. Bars indicate mean ± SE (n = 10), different letters above the bars indicate significant differences at $p < 0.05$.

To further investigate the role of overexpressing *BcAMT1;5*, the ox-6 line was selected as the research object for the subsequent test. Compared with the wild-type, overexpression of *BcAMT1;5* significantly promoted the growth of *Arabidopsis* seedlings under a mixture nutrition of NH_4^+ and NO_3^- (0.0625 mmol L^{-1} NH_4^+ + 0.1875 mmol L^{-1} NO_3^-), and the fresh weight of shoots and roots was 1.24- and 1.34-fold that of the wild-type, respectively (Figure S2A). Furthermore, root morphology indices of ox-6 line seedlings were significantly increased by 1.23- to 1.82-fold of the wild-type, including the length of primary root, the number of lateral roots, and the density of lateral roots (Figure S2B).

The effects of overexpressing *BcAMT1;5* lines on NH_4^+ and NO_3^- uptake and transportation were evaluated under a mixture nutrition of NH_4^+ and NO_3^-, including ion flux rates, N content, and N accumulation in *Arabidopsis* seedlings. As shown in Figure 11A, the ox-6 line had larger net NH_4^+ influxes than that of wild-type (i.e., 1.27-fold of wild-type), while there was little difference in net NO_3^- influxes between the wild-type and ox-6 line. As for N concentration, the NH_4^+ and NO_3^- contents were evidently increased in the ox-6 line. Because of the increase in fresh weight and N content in overexpressing *BcAMT1;5*, the accumulation of NH_4^+ and NO_3^- was significantly enhanced in the ox-6 line compared with those in the wild-type (Figure 11C). Furthermore, the expression levels of related N-assimilation genes were investigated under a mixture of NH_4^+ and NO_3^-. In the roots of overexpressing *BcAMT1;5* line, the expression level of *AtGLN1;1*, encoding GS, was 1.52-fold higher than that of the wild-type, whereas the expression levels of *AtGLN1;2*, *AtGLN2*, and *AtGLT1*, which encoded GOGAT, were significantly decreased, being 0.04– 0.49% of the wild-type (Figure 11D). In leaves, the transcript levels of *AtGLN1;1*, *AtGLN2*, and *AtGDH2*, which encoded glutamate dehydrogenase (GDH), were significantly increased by 3.57–4.58 times those of the wild-type (Figure 11E).

Preprints (www.preprints.org) | NOT PEER-REVIEWED | Posted: 16 November 2022 doi:10.20944/preprints202211.0305.v1

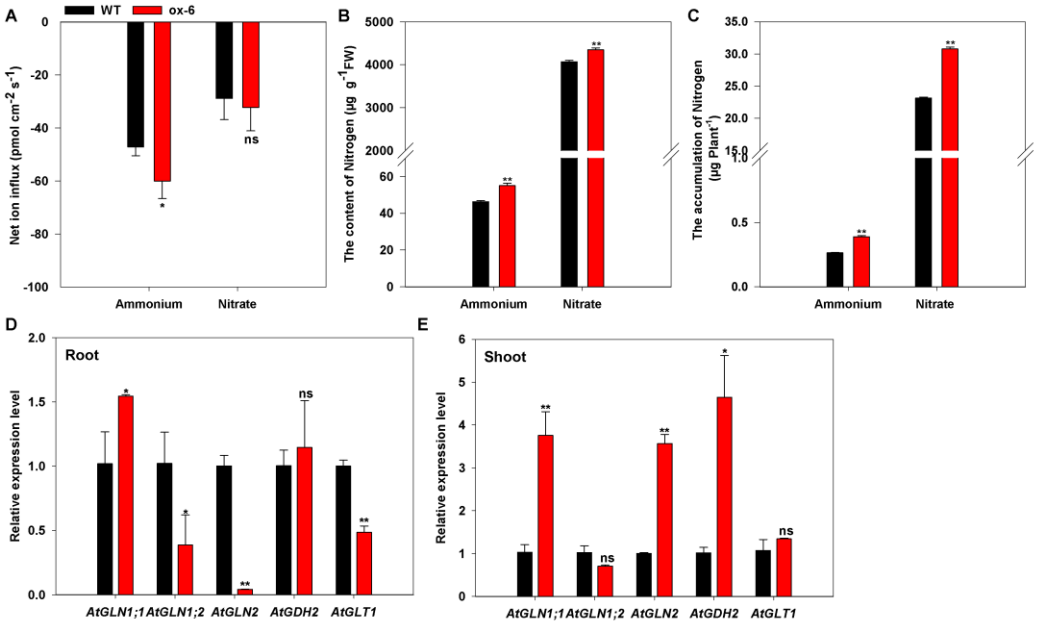

Figure 11. Overexpressing *BcAMT1;5* in *Arabidopsis* improves plant growth at the mixture nutrition of 0.0625 mmol L^{-1} NH_4^+ + 0.1875 mmol L^{-1} NO_3^- as N source. (**A**) Net ion fluxes of NH_4^+ and NO_3^-. (**B**) The content of NH_4^+ and NO_3^-. (**C**) The accumulation of NH_4^+ and NO_3^- . The expression levels of N assimilation genes in roots (**D**) and in shoots (**E**). WT and ox-6 present wild-type and the line6 of overexpressing *BcAMT1;5*, respectively. Data represent mean ± SE (n=16 in A; n=3 in A–E), different letters above the bars indicate significant differences at $p < 0.05$, and ** in the histogram shows significant differences at $p < 0.01$.

3. Discussion

In the present study, we identified one AMT gene, *BcAMT1;5*, from *B. campestris*, which is a member of the AMT1 subfamily. It contains 10 TMs and an AMT1 subfamily signature motif (^{201}DFAGSGVVHMVGGIAGLWGALIEGPR^{226}), which is located in the sixth transmembrane helix, and is conserved among AMT members of *Arabidopsis*, *B. rapa*, and flowering Chinese cabbage (Figure 1). This conserved motif can be used to identify other AMT subfamily members in plant species [17]. The GFP signal of pBI121-BcAMT1;5-GFP protein was mainly located in the plasma membrane (Figure 2). Overexpression of *pYES2-BcAMT1;5* recovered the normal growth of the yeast mutant strain 31019b with 2 mmol L^{-1} NH_4^+ as the sole N source (Figure 3), being similar to AMT members in other plant species [8, 15, 18]. Therefore, *BcAMT1;5* in flowering Chinese cabbage encodes a functional ammonium transporter.

In previous studies, multiple AMT1s genes in *Arabidopsis* [8] and *Malus robusta* [19] showed different spatial expression and NH_4^+ uptake capacity to respond differentially to varying environments and nutritional conditions. Similarly, the results showed that *BcAMT1;5* was mainly expressed in the roots and flowers of flowering Chinese cabbage, but was not expressed or expressed less in the leaves and stems (Figure 4). The first study of AMT1 genes in *Arabidopsis* showed that these genes are transcribed in all major organs, but are highly expressed in roots [20]. However, the opposite results were observed in *M. robusta*; the transcription *of MrAMT1;5* is mainly observed in leaves and stems, and less in roots [19]. The *AMT1;5* gene in apples manifested high transcript levels in mature leaves and young fruits [19]. The expression features of AMTs in different plant species demonstrate intricate tissue specificities, suggesting that they may have distinct physiological functions in NH_4^+ uptake and utilization [13].

Previous studies have shown that the expression patterns of *AMT1* genes in response to different N regimes are common in plants [8, 13, 14, 17, 19]. In this study, *BcAMT1;5* transcription was visibly up-regulated by N starvation, being 5.69-fold in response to N-deficiency treatment for 48 h compared with that at 0 h (Figure 5). Under either N-starvation or normal N levels, supplying different concentrations of NH_4^+ decreased the

Preprints (www.preprints.org) | NOT PEER-REVIEWED | Posted: 16 November 2022 doi:10.20944/preprints202211.0305.v1

transcription of *BcAMT1;5*, with an increase in NH_4^+ concentration under external N conditions (Figure 6A, B). Additionally, adding different ratios of NH_4^+ and NO_3^- distinctly changed the transcript level of *BcAMT1;5*, regardless of N-deficiency or normal N levels (Figure 6C, D). Under normal N conditions, adding lower ratios of NH_4^+ and NO_3^- nutrition increased the expression of *BcAMT1;5* compared with that of other N treatments (Figure 6D). Previous studies have reported that NO_3^- may regulate AMT gene expression to affect cytosolic NH_4^+ homeostasis or participate in more complex feedback responses by affecting plant metabolism [21, 22]. Our previous study reported that BcAMT1;2 may be involved in the interaction between NH_4^+ and NO_3^- [14]. In addition, we measured the GUS activities of *BcAMT1;5*$_{pro}$*::GUS* in response to different N regimes, which was expressed mainly in the vascular tissues of *Arabidopsis* seedlings, up-regulated by N-deficiency and the addition of NO_3^-, and down-regulated by adding NH_4^+ or a mixture of NO_3^- and NH_4^+ (Figure 8). These results indicate that the expression of *BcAMT1;5* in flowering Chinese cabbage was affected by external N status.

It is well known that circadian rhythm is involved in regulating NH_4^+ uptake in plants, and many studies have shown that AMT transcription is correlated with diurnal variation [17, 23, 24]. In agreement with previous results, the expression of *BcAMT1;5* in the roots of flowering Chinese cabbage was strongly affected by diurnal variation, with the highest transcript being found at 12:00 and the lowest ones being found at 21:00–24:00. This indicates that NH_4^+ uptake and assimilation by regulated *AMT* genes might be controlled by carbohydrate availability [15, 17, 23, 25, 26].

To further understand the biological function of BcAMT1;5, we constructed *Arabidopsis* lines overexpressing *BcAMT1*;5. At a low concentration of NH_4^+. The overexpressing *BcAMT1;5* lines accelerated the growth of *Arabidopsis*, which increased NH_4^+ content and ion influxes, compared with that of the wild-type (Figure 9A-E), which is consistent with the overexpression of *AtAMT1;5* in *Arabidopsis* lines [8] and *BcAMT1;2* in *B. campestris* lines [14]. Compared with the wild-type, overexpressing *BcAMT1;5* sharply inhibited seedling growth at 20 mmol L^{-1} of MeA (Figure 10). These results again show that *BcAMT1;5*, isolated from flowering Chinese cabbage, encodes a functional AMT protein. In agreement with a previous study [8], AtAMT1;5 can access external NH_4^+ by uptake across the plasma membrane of rhizodermis cells and is responsible for the residual high-affinity NH_4^+ uptake by AtAMT1;1–AtAMT1;3. The OsAMTs protein can promote rice root branching and root system buildup at low NH_4^+ concentrations [27]. In the mixture of NH_4^+ and NO_3, overexpressing *BcAMT1;5* significantly accelerated the growth of *Arabidopsis* seedlings, with a higher fresh weight and lateral root number, and a longer primary root length, in contrast to that of the wild-type (Figure S2). Additionally, net NH_4^+ influxes were obviously increased, but net NO_3^- influxes were not obviously affected (Figure 11A), and the content and accumulation of NH_4^+ and NO_3^- were higher than those of the wild type (Figure 11B, C), indicating that the constitutive expression of *BcAMT1;5* clearly increased the N influx into roots. Our previous study has reported that *BcAMT1.2*-overexpressing lines increase the net influx of NH_4^+ and reduced that of NO_3^-, especially from net influxes to net effluxes of NO_3^- [14]. Although both BcAMT1;2 and BcAMT1;5 are involved in NH_4^+ uptake, they may have different effects on NO_3^- uptake by flowering Chinese cabbage.

Overexpression *of AMT* genes may change cellular NH_4^+ pools or accumulate excess NH_4^+, which can be toxic to plant cells [28]. If N assimilation can keep up with the increase in NH_4^+ uptake, the detrimental effects of NH_4^+ can be avoided [29]. It is well known that NH_4^+ needs to be assimilated by the GS/GOGAT pathway, the GDH pathway is complementary to NH_4^+ assimilation, and NH_4^+ and 2-oxoglutarate can synthesize glutamate catalyzed by GDH [30]. In *Arabidopsis*, *AtGLN*, *AtGDH*, and *AtGLT* encode GS, GDH, and GOGAT, respectively [30, 31]. In rice, GS activity is essential for plant growth because it supplies amino acids and reduces NH_4^+ toxicity [32]. A previous study reported that the transcription of N assimilation-related genes is regulated by the NH_4^+ status in plants [33]. In this study, the results showed that the transcription of *AtGLN1;1* in roots of the *BcAMT1;5*-overexpressing line was significantly up-regulated in contrast to the wild-type (Figure 11D), while the expression levels of *AtGLN1;1*, *AtGLN2*, and *AtGDH2* were

Preprints (www.preprints.org) | NOT PEER-REVIEWED | Posted: 16 November 2022 doi:10.20944/preprints202211.0305.v1

strongly enhanced in shoots of the *BcAMT1;5* overexpressing line (Figure 11E). Previous studies have reported that *OsAMT1;1* and *OsAMT1;2* overexpressing transgenic plants enhance the expression levels of *OsGS1;1* and *OsGS2;1* and GS activity in rice [34, 36], and our previous study has shown that overexpression of *BcAMT1;2* in *Arabidopsis* up-regulates the transcription of *AtGLN1;2*, *AtGLN2*, *AtGDH2*, and *AtGLT1* [14]. Increased N assimilation gene expression levels or activities would have led to higher rates of assimilation of NH_4^+ to glutamine, avoiding NH_4^+ toxicity [22]. However, in the present study, we observed that the expression of *AtGLN1;2*, *AtGLN2*, and *AtGLT1* was evidently down-regulated in the roots of the *BcAMT1;5*-overexpressing line compared with that in the wild- type (Figure 11D). As a central metabolite of N assimilation, glutamine plays a dual role in the regulation of *ZmAMT1s* in maize, with positive induction under low glutamine levels and negative feedback regulation under high glutamine levels, with the aim of preventing excessive NH_4^+ accumulation in roots [35]. In *Arabidopsis*, excessive NH_4^+ assimilation by GS can cause NH_4^+ toxicity [36]. Therefore, we speculated that the decrease in *AtGLN1;2*, *AtGLN2*, and *AtGLT1* transcripts in the roots of *BcAMT1;5*-overexpressing lines could help avoid NH_4^+ toxicity. These results indicated that different members of the AMTs subfamily may play roles in NH_4^+ uptake and assimilation through different mechanisms. Different AMT1 members are required for NH_4^+ uptake and assimilation [12]. According to the analysis of cis-acting regulatory elements, the sequence of *BcAMT1;5* promoter contained several binding elements about metabolisms (i.e., TATABOX5 for N metabolism, DOFCOREZM for carbon metabolism) and light regulatory elements (i.e., I box, INRNTPSADB) (Table S3). These cis-acting elements might play important roles in the function of BcAMT1;5 regulating N absorption and assimilation.

4. Materials and Methods

4.1. Plant materials and culture conditions

The experiment was conducted in a greenhouse at the South China Agricultural University. Flowering Chinese cabbage (Youlv 501, cultivated by Guangzhou Academy of Agriculture Sciences, Guangdong Province, China) seeds were sterilized and sown in plug trays filled with perlite and then further grown in modified Hoagland solution (4.0 mmol L^{-1} $NaNO_3$, 2.0 mmol L^{-1} KCl, 1.0 mmol L^{-1} KH_2PO_4, 1.0 mmol L^{-1} $MgSO_4$, 0.5 mmol L^{-1} $CaCl_2$, 0.1 mmol L^{-1} Fe-EDTA, 50 μmol L^{-1} H_3BO_3, 12 μmol L^{-1} $MnSO_4$, 1 μmol L^{-1} $CuSO_4$, 1 μmol L^{-1} $ZnCl_2$, and 0.2 μmol L^{-1} Na_2MoO_4). Uniform seedlings at three-leaf heart stage were selected and transplanted to several plastic boxes with modified Hoagland solution. The pH of the nutrient solution was adjusted to 5.8–6.0 every two days, and the nutrient solution was changed every four days. An air pump was installed at 15 min h^{-1} to maintain good air circulation. After transplanting for 40–50 d, roots, functional leaves, young leaves, stems, petioles, and flowers were collected at the flowering stage. After cultivation for 10–15 d, other seedlings were subjected to N-starvation and N-resupply treatments. Seedlings were washed in deionized water and transferred to an N-free modified Hoagland solution containing 4 mmol L^{-1} NaCl instead of 4 mmol L^{-1} $NaNO_3$ for 48 h. During this period, roots and shoots were harvested at 0, 0.5, 1, 2, 4, 24, and 48 h. For the treatments of different N regimes, seedlings that were N-deficient for 48 h and supplied with normal N were transferred to different concentrations of NH_4^+ (i.e., 0.5, 2, 10 mmol L^{-1}) and different ratios of NH_4^+ and NO_3^- (i.e., 0:100, 5:95, 25:75, 50:50, and 100:0) for 2 h, and the samples were harvested. For the circadian rhythm study, seedlings were cultured in a greenhouse (25 to 30 °C, natural light) and then transferred to a growth incubator at 25 °C, 70% relative humidity, 150 μmol m^{-2} s^{-1} light intensity, and a 12/12 h light/dark period (light, 7:00 to 19:00; dark 19:00 to 7:00). After 3 d, leaves and roots were first sampled at 3:00 to 24:00 and then sampled every 3 h. All samples were randomly selected from four plants per biological replicate. All the samples were immediately frozen in liquid nitrogen and stored at –80 °C for quantitative real-time PCR (qPCR).

Preprints (www.preprints.org) | NOT PEER-REVIEWED | Posted: 16 November 2022 doi:10.20944/preprints202211.0305.v1

4.2. Gene cloning and bioinformatics analysis of BcAMT1;5

Based on AMT1;5 sequence of *Brassica rapa* (retrieved from GenBank under accession no. XM_009137637.1) specific primers were designed (Table S1). Total RNA was extracted from the leaves and roots of flowering Chinese cabbage using the Plant RNAiso Plus Kit (TaKaRa, Kyoto, Japan) and was reverse transcribed using the PrimeScript™ 1st Strand cDNA Synthesis Kit (TaKaRa). The open reading frame (ORF) sequence of *BcAMT1;5* was amplified by PCR using cDNA from flowering Chinese cabbage as a template, and the products were ligated into the pCAMBIA3301 vector (Dingguo Biotechnology, Beijing, China) and sequenced.

Based on the deduced amino acid sequences, the following protein characteristics were predicted using online tools: physicochemical properties (ProtParam, http://web.expasy.org/protparam/), PROSITE motifs (ScanProsite, http://prosite.expasy.org/scanprosite/), transmembrane motifs (Protter, http://wlab.ethz.ch/protter/), and sub-cellular localization (http://www.softberry.com). Multiple sequence alignment of 29 AMT proteins from flowering Chinese cabbage (*B. campestris*), *A. thaliana*, *B. rapa*, *Oryza sativa*, and *Populus trichocarpa* were conducted. Phylogenetic analysis based on an unrooted, maximum-likelihood-based phylogenetic tree was conducted using CLUSTALW in MEGA 6.0 [37]. Conserved domains defining the AMT subfamilies were generated using WEBLOGO (http://weblogo.berkeley.edu/logo.cgi/) [38].

4.3. Sub-cellular location

The AMT1;5 primers (Table S1) were used to amplify the coding sequence of *BcAMT1;5*. The amplicons were ligated into the pBI121-GFP vector (kindly provided by Dr. Guibing Hu, South China Agricultural University, China), which harbored the CaMV 35S promoter and GFP, at the *Xba*I and *Sma*I sites. They were then transformed into onion epidermal cells using *Agrobacterium tumefaciens* (EHA105; Weidi Biotechnology, Shanghai, China) infiltration. After two days of incubation, the fluorescence levels of the fusion proteins were examined under a positive fluorescence microscope (Axio Imager D2; Zeiss, Dresden, Germany) at 480 nm excitation and 525 nm emission wavelengths.

4.4. qPCR

Total RNA was extracted from the samples using the Plant RNAiso Plus Kit (TaKaRa) and was reverse transcribed using the PrimeScript™ RT reagent Kit with gDNA Eraser (TaKaRa). The qPCR was performed in a LightCycler 480 Real-Time PCR System (Roche, Basel, Switzerland) using SYBR Premix Ex Taq (TaKaRa) and the primer pairs listed in Table S1. Genes encoding glyceraldehyde-3-phosphate dehydrogenase and β-actin were used as internal controls. The PCR mixture (10 μL total volume) contained 5 μL of 2× SYBR Premix Ex Taq, 0.4 μL of each primer (10 μmol L^{-1}), 2 μL of 10-fold diluted cDNA, and 2.2 μL of ddH_2O. The PCR program was initiated at 95 °C for 30 s, followed by 45 cycles of 95 °C for 5 s and 60 °C for 30 s, and completed with a melting curve analysis (65 to 95 °C, at increments of 0.5 °C), which was conducted to confirm primer specificity. Three biological replicates were used to calculate relative gene expression, as previously described by Livak and Schmittgen [39].

4.5. Yeast growth and complementation

Yeast expression vectors were constructed by cloning the ORF of *BcAMT1;5* into the *Eco*RI and *Xba*I sites of the pYES2 vector (Waryong Biotechnology), respectively. The yeast mutant strain 31019b (*Δmep1*, *Δmep2*, *Δmep3*, and *ura3*), kindly provided by Dr. Bruno André (Université Libre de Bruxelles, Belgium), was unable to grow on medium containing an ammonium concentration lower than 5 mM as the only N source [8]. Recombinant or empty pYES2 plasmids were transformed into 31019b yeast cells using LiAcO [8]. Transformed cells were plated on synthetic dropout medium lacking uracil (FunGenome Company, Beijing, China) to identify positive clones. Positive clones were precultured in liquid yeast N base medium without amino acids (FunGenome Company, Beijing, China), and NH_4^+ was added until an optical density of 1.0 at 600 nm was reached. Growth

Preprints (www.preprints.org) | NOT PEER-REVIEWED | Posted: 16 November 2022 doi:10.20944/preprints202211.0305.v1

complementation assays were performed on solid yeast N base medium at pH 5.8 containing 2% galactose and a single N source (1 mmol L^{-1} arginine or 2 mmol L^{-1} NH_4^+). Overnight cultures were serially diluted by factors of 10, and 3 μL of precultured yeast cell suspensions at each dilution were spotted on yeast N base medium. Growth was evaluated after three days of incubation at 30 °C.

4.6. Construction of pCAMBIA1391-BcAMT1;5$_{pro}$::GUS for Arabidopsis Transformation and glucorinidase (GUS) Assays

The sequence of the *BcAMT1;5* promoter (*BcAMT1;5$_{pro}$*) was amplified by PCR from the DNA of flowering Chinese cabbage using *AMT1;5$_{pro}$* primers (Table S1). They were ligated into the pCAMBIA1391 vector, which harbors *GUS* without any promoter (Dingguo Biotechnology), yielding the *pCAMBIA1391-BcAMT1;5$_{pro}$::GUS* construct. Through *A. tumefaciens*-mediated transformation, empty vector and *BcAMT1;5$_{pro}$::GUS* transgenic plants were generated in a wild-type (Col-0) background. Second-generation (T_2) seeds were germinated on medium containing 1/2 modified Murashige and Skoog Medium (MS, PhytoTech, Kansas, USA), 4 mmol L^{-1} NO_3^-, and 0.7% agar for 14 d (growth conditions as described above). Some seedlings were subjected to N-free MS treatment for 4 d, and then were transferred to either N-free MS or N-free MS containing 0.25 mmol L^{-1} NH_4^+, 0.25 mmol L^{-1} NO_3^-, and a mixture of 0.0625 mmol L^{-1} NH_4^+ and 0.1875 mmol L^{-1} NO_3^- incubated with gentle shaking for 2 h. Histochemical GUS assays were performed as described by Zhu et al. [14]. After histochemical staining, the seedlings were cleared in 70% ethanol and the images were examined under a digital stereo microscope (SMZ171; Shanghai Optical Instrument Factory, Shanghai, China).

4.7. Generation of BcAMT1;5-expressing Arabidopsis transgenic lines

Wild-type *Arabidopsis* (Col-0) was transformed with *Agrobacterium* GV1301 harboring pCAMBIA3301-35S$_{pro}$::*BcAMT1;5*::NOS$_{term}$ by flower bud dipping [40], and several transformants were selected by phosphinothricin-resistance, PCR test using bar primers, and qPCR test of leaves using special *BcAMT1;5* primers (Table S1). Independent homozygous *BcAMT1;5*-transformed lines were created in the T4 generation. Three lines were used in the experiment of growth phenotyping, and one line was used for ion fluxes, N content, N accumulation, and gene expression.

4.8. Plant Culture for Growth Test, NH_4^+ Uptake, Ion Fluxes and Gene Expression

For the growth test, surface-sterilized *Arabidopsis* seeds were germinated on half-strength MS agar medium (containing 4 mmol L^{-1} NO_3^- as the N source) for 4 d, and seedlings were then transferred to vertical plates containing half-strength MS with 0.25 mmol L^{-1} NH_4^+ for 10 d. Seedlings were harvested to measure the biomass, primary root length, and NH_4^+ content. The NH_4^+ content was measured as described by Ivančič and Degobbis [41]. The NH_4^+ and NO_3^- ion fluxes were measured by scanning ion-selective electrode technique (MA01002 system; Younger USA Science and Technology Limited Liability, Amherst, MA, USA) according to Zhu et al. [14]. This work was performed at Xuyue Science and Technology Limited Company (Beijing, China). Six similar seedlings from each treatment were selected for ion flux analyses. For the NH_4^+ toxic analog, methylammonium (MeA), the consistent seedlings were transferred to vertical plates containing 20 mmol L^{-1} MeA for 10 d. For the responses to a mixture of N nutrition, *Arabidopsis* seeds were precultured for 7 d, and then transformed into half-strength MS agar medium (containing 0.0625 mmol L^{-1} NH_4^+ + 0.1875 mmol L^{-1} NO_3^-) for 7 d. The content and accumulation of NH_4^+ and NO_3^- were determined as described by Ivančič and Degobbis [41]. Shoots and roots were harvested for total RNA isolation and qPCR.

4.9. Statistical analysis

Data from three independent experiments were analyzed by Microsoft excel (Microsoft Corporation, Washington, USA) and SPSS 21 (SPSS Incorporation, Chicago, USA). Figures were drawn by SigmaPlot (11.1) (Jandel Scientific software, San Rafael, CA, USA),

 doi:10.20944/preprints202211.0305.v1

and differences were compared using Duncan's test by SPSS 21, with $p < 0.05$ or $p < 0.01$ as the significance threshold.

5. Conclusions

In this study, we identified and characterized *BcAMT1;5* from flowering Chinese cabbage. The gene has a highly conserved signatural motif of the AMT1 subfamily. The expression features demonstrated that *BcAMT1;5* is mainly expressed in the roots of flowering Chinese cabbage and may participate in NH_4^+ transport into specific tissues. Additionally, *BcAMT1;5* showed multiple transcript patterns of different N regimes in response to varying nutritional conditions in the environment, which were up-regulated by N-deficiency and down-regulated by supplying NH_4^+. The GUS activities of *BcAMT1;5*$_{pro}$*::GUS* overexpressing lines showed similar changes in response to different N conditions. Furthermore, at low N concentrations, overexpression of *BcAMT1;5* accelerated seedling growth, increased N influx, and increased N content in contrast to that in the wild-type. This suggests that transcriptional regulation of *BcAMT1;5* in flowering Chinese cabbage may participate in N uptake and assimilation under various N conditions. Therefore, further studies will be conducted in the future to investigate the molecular mechanisms that link AMT members and the uptake and assimilation of N in response to different N supplies.

Supplementary Materials: Table S1: Primer sequences used in this study; Table S2: The sequence information for each AMT protein used for the phylogenetic analysis; Figure S1: Identification of qPCR in different *BcAMT1;5*-overexpressing lines; Figure S2: Overexpression *of BcAMT1;5* in *Arabidopsis* improves plant growth with a mixture of 0.0625 mmol L^{-1} NH_4^+ and 0.1875 mmol L^{-1} NO_3^- as the N source; Table S3: The prediction analysis of regulatory elements for the promoter of *BcAMT1;5*.

Author Contributions: Conceptualization, S.S. and C.R.; methodology, Z.Y. and Z.L.; data analysis, H.X. and Z.Y.; writing—original draft preparation, Z.Y. and Z.L.; writing—review and editing, Z.Y. and Z.L.; revision, S.W., S.G., and L.H.; funding acquisition, C.R., S.S., and Z.Y. All authors have read and approved the content of the manuscript.

Funding: This work was supported by the National Natural Science Foundation of China (31972481 and 32072656), the Natural Science Foundation of Guangdong Province, China (2019A1515011680), the Guangdong Provincial Special Fund for Modern Agriculture Industry Technology Innovation Teams (2022KJ131), the Characteristic Innovation Project of Guangdong Provincial Department of Education (2019KTSCX164), and the Science and Technology Research Project of Shaoguan, Guangdong Province (200810224537535).

Data Availability Statement: Not applicable

Acknowledgments: We thank Dr. Guibing Hu from South China Agricultural University for kindly providing the pBI121-GFP vector, and Dr. Bruno Andre from Universite Libre de Bruxelles for kindly providing the yeast mutant strain 31019b.

Conflicts of Interest: The authors declare no conflicts of interest

References

1. Gu, J.; Yang, J. Nitrogen (N) transformation in paddy rice field: Its effect on N uptake and relation to improved N management. *Crop and Environment* **2022**, 1, 7–14. https://doi.org/10.1016/j.crope. 2022.03.003.
2. Bloom, A.J.; Burger, M.; Asensio, J.S.R.; Cousins, A.B. Carbon dioxide enrichment inhibits nitrate assimilation in wheat and *Arabidopsis*. *Science* **2010**, 328, 899–903. https://doi.org/ 10.1126/ science.1186440.
3. Wang, Y.; Zhou, W.; Wu, J.; Xie, K.; Li, X. LjAMT2;2 Promotes ammonium nitrogen transport during arbuscular mycorrhizal fungi symbiosis in *Lotus japonicus*. *Int. J. Mol. Sci.* **2022**, 23, 9522. https://doi.org/10.1515/biol-2022-0084.
4. Gazzarrini, S.; Lejay, L.; Gojon, A.; Ninnemann, O.; Frommer, W.B.; von Wiren, N. Three functional transporters for constitutive, diurnally regulated, and starvation-induced uptake of ammonium into *Arabidopsis* roots. *Plant Cell* **1999**, 11, 937–948. https://doi.org/10.1105/tpc.11.5. 937.
5. Hao, D.; Yang, S.; Huang, Y.; Su, Y. Identification of structural elements involved in fine-tuning of the transport activity of the rice ammonium transporter OsAMT1;3. *Plant Physiol. Bioch.* **2016**, 108, 99–108. https://doi.org/10.1016/j.plaphy.2016.07.003.
6. Hao, D.; Zhou, J.; Yang, S.; Qi, W.; Yang, K.; Su, Y. Function and regulation of ammonium transporters in plants. *Int. J. Mol. Sci.* **2020**, 21, 3557. https://doi.org/10.3390/ijms21103557.
7. McDonald, T. R.; Ward, J. M. Evolution of electrogenic ammonium transporters (AMTs). *Front. Plant Sci.* **2016**, 7. https://doi.org/10.3389/fpls.2016.00352.
8. Yuan, L.; Loqué, D.; Kojima, S.; Rauch, S.; Ishiyama, K.; Inoue, E.; Takahashi, H.; von Wirén, N. The organization of high-affinity ammonium uptake in *Arabidopsis* roots depends on the spatial arrangement and biochemical properties of AMT1-Type transporters. *Plant Cell* **2007**, 19, 2636–2652. https://doi.org/10.1105/tpc.107.052134.
9. Yuan, L.; Graff, L.; Loqué, D.; Kojima, S.; Tsuchiya, Y. N.; Takahashi, H.; von Wirén, N. AtAMT1;4, a pollen-specific high-affinity ammonium transporter of the plasma membrane in *Arabidopsis. Plant Cell Physiol.* **2009**, 50, 13–25. https://doi.org/10.1093/pcp/pcn186.
10. Nacry, P.; Bouguyon, E.; Gojon, A. Nitrogen acquisition by roots: physiological and developmental mechanisms ensuring plant adaptation to a fluctuating resource. *Plant Soil* **2013**, 370, 1–29. https://doi.org/10.1007/s11104-013-1645-9.
11. Ijato, T.; Porras Murillo, R.; Ganz, P.; Ludewig, U.; Neuhäuser, B. Concentration-dependent physiological and transcriptional adaptations of wheat seedlings to ammonium. *Physiol. Plantarum* **2021**, 171, 328–342. https://doi.org/10.1111/ppl.13113.
12. Konishi, N.; Ma, J. F. Three polarly localized ammonium transporter 1 members are cooperatively responsible for ammonium uptake in rice under low ammonium condition. *New Phytol.* **2021**, 232, 1778–1792. https://doi.org/10.1111/nph.17679.
13. Huang, L.; Li, J.; Zhang, B.; Hao, Y.; Ma, F. Genome-wide identification and expression analysis of AMT gene family in apple (*Malus domestica* Borkh.). *Horticulturae* **2022**, 8, 457. https://doi.org/ 10.3390/horticulturae8050457.
14. Zhu, Y.; Huang, X.; Hao, Y.; Su, W.; Liu, H.; Sun, G.; Chen, R.; Song, S. Ammonium transporter (BcAMT1.2) mediates the interaction of ammonium and nitrate in *Brassica campestris*. *Front. Plant Sci.* **2020**, 10. https://doi.org/10.3389/fpls.2019.01776.
15. Zhong, L.; Huang, X.; Zhu, Y.; Kou, E.; Liu, H.; Sun, G.; Chen, R.; Song, S. Characterization and expression analysis of BcAMT1;4, an ammonium transporter gene in flowering Chinese cabbage. *Hortic. Environ. Biotechnol.* **2019**, 563–572. https://doi.org/10.1007/s13580-019-00155-3.
16. Ludewig, U. Ion transport versus gas conduction: function of AMT/Rh-type proteins. *Transfus. Clin. Biol.* **2006**, 13, 111–116. https://doi.org/10.1016/j.tracli.2006.02.012.

17. Couturier, J.; Montanini, B.; Martin, F.; Brun, A.; Blaudez, D.; Chalot, M. The expanded family of ammonium transporters in the perennial poplar plant. *New Phytol.* **2007**, 174, 137–150. https://doi.org/10.1111/j.1469-8137.2007.01992.x.

18. Li, H.; Han, J.; Chang, Y.; Lin, J.; Yang, Q. Gene characterization and transcription analysis of two new ammonium transporters in pear rootstock *(Pyrus betulaefolia*). *J. Plant Res.* **2016**, 129, 737–748. https://doi.org/10.1007/s10265-016-0799-y.

19. Li, H.; Yang, Q.S.; Liu, W.; Lin, J.; Chang, Y.H. The AMT1 family genes from *Malus robusta* display differential transcription features and ammonium transport abilities. *Mol. Biol. Rep.* **2017**, 44, 379–390. https://doi.org/10.1007/s11033-017-4119-y.

20. Ninnemann, O.; Jauniaux, J.C.; Frommer, W. B. Identification of a high affinity NH_4^+ transporter from plants. *EMBO J.* **1994**, 13, 3464–3471. https://doi.org/10.1002/j.1460-2075.1994.tb06652.x.

21. Hachiya, T.; Sakakibara, H. Interactions between nitrate and ammonium in their uptake, allocation, assimilation, and signaling in plants. *J. Exp. Bot.* **2017**, 68, 2501–2512. https://doi.org/10.1093/jxb/erw449.

22. Jian, S.; Liao, Q.; Song, H.; Liu, Q.; Lepo, J.E.; Guan, C.; Zhang, J.; Ismail, A.M.; Zhang, Z.; Abdelbagi, M. et al. NRT1.1-related NH_4^+ toxicity is associated with a disturbed balance between NH_4^+ uptake and assimilation. *Plant Physiol.* **2018**, 178, 1473–1488. https://doi.org/10.1104/pp.18.00410.

23. Li, H.; Cong, Y.; Chang, Y.; Lin, J. Two AMT2-Type ammonium transporters from pyrus betulaefolia demonstrate distinct expression characteristics. *Plant Mol. Biol. Rep.* **2016**, 34, 707–719. https://doi.org/10.1007/s11105-015-0957-8.

24. Hachiya, T.; Mizokami, Y.; Miyata, K.; Tholen, D.; Watanabe, C.K.; Noguchi, K. Evidence for a nitrate-independent function of the nitrate sensor NRT1.1 in *Arabidopsis thaliana*. *J. Plant Res.* **2011**, 124, 425-430. https://doi.org/10.1007/s10265-010-0385-7.

25. Camañes, G.; Cerezo, M.; Primo-Millo, E.; Gojon, A.; García-Agustín, P. Ammonium transport and *CitAMT1* expression are regulated by N in Citrus plants. *Planta* **2009**, 229, 331–342. https://doi.org/10.1007/s00425-008-0833-y.

26. Zhu, Y.; Hao, Y.; Liu, H.; Sun, G.; Chen, R; Song, S. Identification and characterization of two ammonium transporter genes in flowering Chinese cabbage (*Brassica campestris*). *Plant Biotechnol.* **2018**, 35, 59–70. https://doi.org/10.3389/fpls.2019.01776.

27. Luo, L.; Zhu, M.; Jia, L.; Xie, Y.; Wang, Z.; Xuan, W. Ammonium transporters cooperatively regulate rice crown root formation responding to ammonium nitrogen. *J. Exp. Bot.* **2022**, 73, 3671–3685. https://doi.org/10.1093/jxb/erac059.

28. Bittsánszky, A.; Pilinszky, K.; Gyulai, G.; Komives, T. Overcoming ammonium toxicity. *Plant Sci.* **2015**, 231, 184–190. https://doi.org/10.1016/j.plantsci.2014.12.005.

29. Liu, Y.; von Wirén, N. Ammonium as a signal for physiological and morphological responses in plants. *J. Exp. Bot.* **2017**, 68, 2581–2592. https://doi.org/10.1093/jxb/erx086.

30. Guan, M.; Thomas, C.D.B.; Carsten, P.; Schjoerring, J.K. Cytosolic glutamine synthetase Gln1;2 is the main isozyme contributing to GS1 activity and can be up-regulated to relieve ammonium toxicity. *Plant Physiol.* **2016**, 1921–1933. https://doi.org/10.1104/pp.16.01195.

31. Pereira, E.G.; Sperandio, M.V.L.; Santos, L.A.; Bucher, C.A.; Coelho, C.P.; Fernandes, M.S. Rice varieties with contrasting nitrogen use efficiency present different expression of amino acid transporters and ammonium transporters. *Arch. Agron. Soil Sci.* **2022**, 1–15. https://doi.org/10.1080 /03650340.2022.2080198.

32. Ranathunge, K.; El-kereamy, A.; Gidda, S.; Bi, Y.; Rothstein, S.J. *AMT1;1* transgenic rice plants with enhanced NH_4^+ permeability show superior growth and higher yield under optimal and suboptimal NH_4^+ conditions. *J. Exp. Bot.* **2014**, 65, 965–979. https://doi.org/10.1093/jxb/ert458.

33. Lee, S.; Marmagne, A.; Park, J.; Fabien, C.; Yim, Y.; Kim, S.J.; Kim, T.H.; Lim, P.O.; Masclaux Daubresse, C.; Nam, H.G. Concurrent activation of *OsAMT1;2* and *OsGOGAT1* in rice leads to enhanced nitrogen use efficiency under nitrogen limitation. *Plant J.* **2020**, 103, 7–20. https://doi.org/10.1111/tpj.14851.

34. The, S.V.; Snyder, R.; Tegeder, M. Targeting nitrogen metabolism and transport processes to improve plant nitrogen use efficiency. *Front. Plant Sci.* **2021**, 11. https://doi.org/10.3389/fpls. 2020. 628366.

35. Hui, J.; Liu, Z.; Duan, F.; Zhao, Y.; Li, X.; An, X.; Wu, X.; Yuan, L. Ammonium-dependent regulation of ammonium transporter *ZmAMT1s* expression conferred by glutamine levels in roots of maize. *J. Integr. Agr.* **2022**, 21, 2413–2421. http:// doi.org/10.1016/S2095-3119(21)63753-X.

36. Hachiya, T.; Inaba, J.; Wakazaki, M.; Sato, M.; Toyooka, K.; Miyagi, A.; Kawai-Yamada, M.; Sugiura, D.; Nakagawa, T.; Kiba, T.et al. Excessive ammonium assimilation by plastidic glutamine synthetase causes ammonium toxicity in *Arabidopsis thaliana*. *Nat. Commun.* **2021**, 12, 4944. https://doi.org/10.1038/s41467-021-25238-7.

37. Tamura, K.; Stecher, G.; Peterson, D.; Filipski, A.; Kumar, S. MEGA6: Molecular Evolutionary genetics analysis version 6.0. *Mol. Biol. Evol.* **2013**, 30, 2725–2729. https://doi.org/10.1093/ molbev/mst197.

38. Crooks, G.E.; Hon, G.; Chandonia, John-Marc; Brenner S.E. WebLogo: A sequence logo generator. *Genome Reserch* **2004**, 14, 1188–1190. https://doi.org/10.1101/gr.849004.

39. Livak, K.J.; Schmittgen, T.D. Analysis of relative gene expression data using real-time quantitative PCR and the $2^{-\Delta\Delta CT}$ method. *Methods* **2001**, 25, 402–408. https://doi.org/10.1006/meth.2001.1262.

40. Wiktorek-Smagur, A.; Hnatuszko-Konka, K.; Kononowicz, A. K. Flower bud dipping or vacuum infiltration-two methods of *Arabidopsis thaliana* transformation. *Russ. J. Plant Physl.* **2009**, 56, 560–568. https://doi.org/10.1134/S1021443709040177.

41. Ivančič, I.; Degobbis, D. An optimal manual procedure for ammonia analysis in natural waters by the indophenol blue method. *Water Res.* **1984**, 18, 1143–1147. https://doi.org/10.1016/0043-1354(84)90230-6.